Forced degradation of cell-based medicinal products guided by flow imaging microscopy: explorative studies with Jurkat cells

Grabarek, A.D.; Jiskoot, W.; Hawe, A.; Pike-Overzet, K.; Menzen, T.

European Journal of Pharmaceutics and Biopharmaceutics 167 (2021) 38–47

Contents lists available at ScienceDirect

European Journal of Pharmaceutics and Biopharmaceutics

journal homepage: www.elsevier.com/locate/ejpb

Forced degradation of cell-based medicinal products guided by flow imaging microscopy: Explorative studies with Jurkat cells

A.D. Grabarek [a,b], W. Jiskoot [a,b,*], A. Hawe [b], K. Pike-Overzet [c], T. Menzen [b,*]

[a] Coriolis Pharma, Fraunhoferstraße 18 b, 82152 Martinsried, Germany
[b] Leiden Academic Centre for Drug Research, Leiden University, the Netherlands
[c] Department of Immunology, Leiden University Medical Center, Leiden, the Netherlands

ARTICLE INFO

Keywords:
Cell-based medicinal products
Cell viability
Debris
Dimethyl sulfoxide
Flow imaging microscopy
Forced degradation
Formulation
Stability

ABSTRACT

Cell-based medicinal products (CBMPs) offer ground-breaking opportunities to treat diseases with limited or no therapeutic options. However, the intrinsic complexity of CBMPs results in great challenges with respect to analytical characterization and stability assessment. In our study, we submitted Jurkat cell suspensions to forced degradation studies mimicking conditions to which CBMPs might be exposed from procurement of cells to administration of the product. Flow imaging microscopy assisted by machine learning was applied for determination of cell viability and concentration, and quantification of debris particles. Additionally, orthogonal cell characterization techniques were used. Thawing of cells at 5 °C was detrimental to cell viability and resulted in high numbers of debris particles, in contrast to thawing at 37 °C or 20 °C which resulted in better stability. After freezing of cell suspensions at −18 °C in presence of dimethyl sulfoxide (DMSO), a DMSO concentration of 2.5% (v/v) showed low stabilizing properties, whereas 5% or 10% was protective. Horizontal shaking of cell suspensions did not affect cell viability, but led to a reduction in cell concentration. Fetal bovine serum (10% [v/v]) protected the cells during shaking. In conclusion, forced degradation studies with application of orthogonal analytical characterization methods allow for CBMP stability assessment and formulation screening.

1. Introduction

The number of cell-based medicinal products (CBMPs) entering clinical trials and being approved by major regulatory bodies for commercial use is consistently increasing each year [1]. Despite the promising clinical data emerging from the use of these innovative therapeutic products, many challenges remain in the areas of manufacturing, formulation development and analytical characterization [2,3].

Most CBMPs consist of living cells, which are intrinsically fragile and much more susceptible to unfavourable conditions compared to other biotherapeutics, such as protein-based products. Nonetheless, irrespective of the type of the CBMP (e.g., autologous or allogenic, genetically modified or not), they often undergo multiple and complex manufacturing steps before being administered to the patient. The main processing steps CBMPs undergo during their production include isolation of cells from a healthy donor or patient, *ex-vivo* cell manipulation, formulation, storage, and quality control prior to release and administration [4]. Furthermore, between each of the above listed steps, transportation, freeze-thawing or manual handling of CBMPs occurs. With clinical site-specific handling procedures, differences in processing and administration of the product will also occur [5]. Such diverse and multistep production and handling processes expose cells to a range of intended and/or accidental environmental stress factors, such as freeze-thawing, surface related stress (i.e., mechanical stress), thermal and oxidative stress. Each of these kinds of stresses may result in accidental cell death or alterations in cell activity. Therefore, examination of the impact of formulation parameters on cell stability under these stress conditions should be considered to better understand the sensitivity of the product to the stress factors involved. This will likely contribute to new insights that can be employed to mitigate the potential risk of therapeutic failure and the occurrence of serious adverse effects due to poor product quality [6,7].

Introduction or formation of particulate impurities in CBMPs is one of the potential risks associated with manufacturing and handling of these drug products [3,8,9]. Particles found in CBMPs can originate from either the process or the cell product itself. Process-related particulate

* Corresponding authors at: Division of BioTherapeutics, Leiden Academic Centre for Drug Research (LACDR), Leiden University, Einsteinweg 55, 2333 CC Leiden, the Netherlands (W. Jiskoot) and Coriolis Pharma, Fraunhoferstraße 18 b, 82152 Martinsried, Germany (T. Menzen).
E-mail addresses: w.jiskoot@lacdr.leidenuniv.nl (W. Jiskoot), tim.menzen@coriolis-pharma.com (T. Menzen).

https://doi.org/10.1016/j.ejpb.2021.07.004
Received 14 April 2021; Received in revised form 30 June 2021; Accepted 10 July 2021
Available online 16 July 2021

impurities may include ineffectively removed antibody coated magnetic beads used for activation and expansion of cells, viral vectors utilized in a cell transduction step, extrinsic particles (glass, cellulose, rubber), or leachables derived from primary containers [10–13]. Sterile filtration of cell suspensions is not possible because of the inherent size of cells; therefore, unwanted micrometer-sized particles will remain in the product if their removal is not complete [14]. Cell-based impurities, on the other hand, comprise materials originating from cells. These may be non-viable or non-therapeutic cells [15], as well as cell agglomerates and cellular debris [9,16]. For example, accidental cell death induced in cells exposed to extreme physiological conditions (pyroptosis) leads to plasma membrane rupture, release of intracellular contents and formation of debris particles [17]. In contrast to apoptotic cell death, where cellular components are packaged into vesicles and digested by appropriate caspases for facilitated removal by the immune system [18], accidental cell death produces debris with potent inflammatory properties. One of the results from these debris particles may be an adverse immune response upon administration [19]. Furthermore, if larger micrometer-sized particles are introduced into the smaller blood vessels, they may result in tissue damage from thromboembolism [20].

Forced degradation studies are commonly included in the development of any pharmaceutical product as part of establishment of analytical methods and formulation screenings [21,22]. Alongside real time stability studies at the intended storage conditions, forced degradation studies are applied to estimate the shelf-life of products as well as define suitable storage and handling conditions [23]. Moreover, this type of studies can simulate accidental exposure of drug products to deleterious conditions and assist in the evaluation of potential risks occurring to drug products throughout their product life-cycle. These studies also assist in selecting appropriate excipients during formulation development where the aim is to determine a component mixture achieving maximum stability for the active pharmaceutical ingredient. Even though the manufacturability, critical quality attributes (CQAs), degradation pathways and product degradants in CBMPs will vary substantially from, e.g., protein-based therapeutics, the same concept of forced degradation studies can be highly relevant in process and product development of CBMPs.

Extensive testing of a CBMP prior to administration to a patient is a regulatory obligation to assure the product is safe, efficacious and of good quality. The testing parameters include identity, purity, activity and potency of cells. However, also cellular and non-cellular materials must be identified and qualified [15,24]. For this purpose, reliable analytical methods for characterization of product quality and stability testing are necessary [25]. In this study we utilized flow imaging microscopy coupled with convolutional neural networks (FIM-CNN) to establish a high-throughput and label free method for quantification of viable and dead cells as well as debris particles in the size range from 1 to 50 μm. Jurkat cells were selected as a model for T cells, such as CAR-T cells [2], in this study. We submitted Jurkat cell suspensions to external stress factors, which allowed us to define the impact of thawing temperature, freeze–thaw stress and shaking stress on the stability of Jurkat cells. In addition to FIM-CNN, we measured cell quality attributes, including cell membrane integrity and cell metabolism, after exposure of the cells to the same stress stimuli.

2. Materials and methods

2.1. Materials

T-cell leukemia cells (Jurkat, Clone E6-1, ATCC® TIB152™) were donated by Leiden University Medical Centre (LUMC) as frozen 1-ml aliquots at a total cell concentration of $1x10^7$ cells/ml (cells counted using NucleoCounter3000 [Chemometec]), and were stored at −145 °C prior to usage. For cryopreservation, Jurkat cells were formulated in high-glucose RPMI 1640 (RPMI medium; ThermoFisher, Waltham, USA) supplemented with 10% (v/v) fetal bovine serum (FBS; Life Technologies, USA) and 10% (v/v) dimethyl sulfoxide (DMSO) (Life Technologies, Carlsbad, USA). Cryopreservation was performed by placing cryogenic vials with Jurkat cell suspensions in a controlled rate freezing apparatus container and cooling with a decreasing temperature at ca. 1 °C per min. Frozen cell suspensions were transferred to liquid nitrogen until shipment. After thawing, removal of FBS and DMSO was performed by dilution of cell aliquots in RPMI medium (at least 40-fold dilution), centrifugation for 10 min at 350 × g and further removal of the supernatant. The cell pellet was resuspended in RPMI medium, 1x phosphate buffered saline (Gibco™, pH, 7.4; ThermoFisher, Waltham, USA) or stain buffer (containing FBS, FisherScientific, New Hampshire, USA) as required. FBS (heat inactivated, sterile-filtered) and DMSO (suitable for hybridoma, ≥ 99.7%) were purchased from Sigma-Aldrich (St. Louis, USA). Dead Cell Apoptosis Kit (annexin V, fluorescein isothiocyanate [FITC] and propidium iodide [PI]), calcein AM dye and CyQUANT™ LDH kit were purchased from (ThermoFisher, Waltham, USA).

2.2. Forced degradation studies

Jurkat cells were exposed to three types of forced degradation studies, as described below. Each of the three types of stress conditions were carried out in duplicate on different days.

2.2.1. Thawing as stress factor

Single 1-ml frozen cell aliquots were transferred from storage at −145 °C on dry ice to a water bath (GFL, Burgwedel, Germany) for thawing at 37 °C for 1 min 30 sec (the default thawing condition). For investigation of other thawing temperatures, cells were also thawed in a water bath at 25 °C for 2 min 40 sec and at 5 °C for 4 min 25 sec. Thawing in the water bath was performed to solely dissolve the ice adhering to the walls of the cryovials. Further, the 1-ml aliquot of the partially frozen cell suspension was transferred into 40 ml of RPMI medium equilibrated to the thawing temperature, where the remaining of the ice nucleus dissolved within seconds. The cell suspension was centrifuged at 350 × g for 10 min at 20 °C, after which the supernatant was discarded and the pellet was resuspended in 5 ml of RPMI medium. Total cell concentration and viability were assessed by using a CASY counter (Bremen, Germany) and dilution to $1x10^6$ cells/ml was performed by addition of the required volume of RPMI medium (containing DMSO or FBS where stated).

2.2.2. Freeze-thaw stress

DMSO, cooled on wet ice, was slowly added to cell suspensions (placed on wet ice) to reach a target concentration 1%, 2.5%, 5% and 10% (v/v) at a cell concentration of $1x10^6$ cells/ml. Further, five 1-ml aliquots were prepared in 1.8-ml Nalgene cryovials, which were submitted to freezing at −18 °C for 3 h. This period of time was sufficient for complete freezing of the aliquots. Prior to analysis, the samples were thawed for 2 min at 37 °C, pooled and washed with fresh RPMI medium. Control samples were stored at 20 °C for 3 h and were otherwise treated identically as the freeze-thawed samples.

2.2.3. Shaking stress

Cells at a concentration of $1x10^6$ cells/ml (without or with FBS at 10% [v/v]) were filled (1 ml) into five Nalgene cryovials (ThermoScientific, Waltham, USA) with a 1.8 ml volume capacity. The cryovials were submitted to shaking by constant horizontal agitation at 185 rpm at 25 °C by using an IC 4000 shaker (IKA, Germany). Analysis of cell suspensions of pooled cell aliquots was performed following 3 h of shaking. Control samples were stored statically and protected from light at 25 °C in cryovials, and subsequently pooled.

2.3. Flow imaging microscopy (FIM)

Cells (viable and dead) and debris particles were quantified by using

a FlowCam 8100 (Fluid Imaging Technologies, Scarborough, USA) equipped with a 50-μm flow cell. The objective used resulted in a 20x magnification and sample imaging was performed by a high-resolution CMOS camera (1920x1200 pixels) at 27 frames per second. In total, a sample volume of 140 μl was measured with an efficiency of approximately 63% (i.e., the imaged sample volume was ca. 87 μl). Particles imaged within the flow cell were detected with intensity thresholds of 12 for light and dark pixels. Cleaning steps between sample measurements involved thorough flushing of the flow cell with Terg-a-zyme® enzyme detergent (1% [w/v]) and highly purified water. Collected images were not sorted by using any morphological filters and samples were measured in triplicate, unless otherwise stated.

2.4. Image analysis using convolutional neural networks

Particle images captured with a FlowCam were analyzed by using convolutional neural networks (CNN). The CNN was based on the VGG-19 architecture described in our previous study [26]. Briefly, the VGG-19 network using rectified linear unit activation functions, punctuated with max-pooling and dropout layers, was pre-trained on a ImageNet dataset discussed in detail elsewhere [27]. The re-training of the network was performed with the first ten layers frozen in order to save computation time and improve accuracy of the model by preserving its pre-learned feature recognition capabilities. For fine-tuning we split our dataset into an 8:1:1 ratio for training, validation and testing, respectively. The model was optimized by running 19 epochs with a stochastic gradient descent optimization algorithm and a 0.001 learning rate. The machine learning model was performed by using Keras (2.2.4), Tensorflow (1.13.1) and Python (3.7.3) libraries, and ran on a Nvidia Turing GPU with 11 GB of VRAM.

2.4.1. Generation of particle images for population discrimination

The CNN was fine-tuned on manually labeled images (4,000–4,500) of each of the three populations: viable cells, dead cells and debris particles.

Images of viable cells were manually selected from measured samples consisting of Jurkat cells with a viability of 86.8% (based on PI assay). For selection of dead cells, two separate methods were used to induce cell death. Firstly, FlowCam images of cell suspensions treated by heat (55 °C for 90 min) were collected, which showed a viability of 7.6% (based on PI assay). Secondly, cells were imaged after incubation with ethanol (10% (v/v)) for 90 min at 37 °C and had a determined viability of 12.8% (based on PI assay). In order to further define image populations of viable and dead cells for the network fine-tuning, morphological parameters, such as aspect ratio, circle fit, convexity, sigma intensity and symmetry, of the two populations were used. Only particles (cells) of morphological parameter values falling between the 10th and 90th percentile of the manually selected population as viable and dead cells were taken for input to the training of the model. Images of debris particles were manually selected from measured suspensions of cells submitted to vortexing for approximately 2 min or two freeze–thaw cycles (−140 °C to 37 °C).

2.5. Automated cell counting

A CASY TTC 150 (Omni Life Science, Bremen, Germany) cell counter equipped with a 150-μm capillary was used for automated cell counting. Cells were diluted 100-fold in CASYton (Omni Life Science, Bremen, Germany) shortly before analysis. Samples were measured in duplicate and each measurement consisted of 5 sub-runs of 400 μl, resulting in >5,000 events counted per analysis.

2.6. Imaging flow cytometry

To assess cell viability based on cell metabolism, imaging flow cytometry was used in combination with the membrane-permeable dye calcein-AM (calcein-AM assay), at a final concentration of 6.3 nM in the sample to be analyzed. After dye addition, cells were incubated at room temperature for 30 min (in the dark) and further washed with 200 μl of stain buffer (with FBS; BD Bioscience, New Jersey, USA). Subsequently, samples were analyzed by using an Amnis FlowSight imaging flow cytometer (Luminex, Seattle, USA) and data were analyzed by using IDEAS 6.2.183 (Luminex, Seattle, USA) image analysis software. Sample measurements were carried out by using a 20× magnification objective in medium-sensitivity mode (132 mm/sec). The side scatter laser was set to 10 mW and the 488-nm fluorescence excitation laser was set to 12 mW. Images of the calcein-AM stained cells were recorded in channel 02 (532/55 nm). Brightfield acquisition was set to channel 9 (582/25 nm) with automatically set intensities. Only particles with a Gradient RMS > 30 were collected as true events. Appropriate morphological filters were applied to discriminate between cells and debris particles, in order to assess cell viability/cell death on the cell population only. Cell viability was calculated based on the proportion of viable cells from the total population shown in Fig. S1. Each measurement was performed in duplicate.

Cell apoptosis and death were determined by imaging flow cytometry after labelling of the cells with annexin V-FITC and PI assays. Sample preparation was carried out according to the Dead Cell Apoptosis Kit instructions. After incubation for 15 min in the dark at room temperature samples were kept on wet ice until analysis. After adjusting the excitation power of the FlowSight imaging flow cytometer to 4 mW, the same instrument settings as described in for the calcein-AM assay above was used. Brightfield as well as fluorescence images in channels 02 (532/55 nm) for annexin V-FITC and channel 04 (610/30 nm) for PI were recorded. Appropriate morphological filters based on mean intensity, area, aspect ratio and modulation from channel 09 were applied to discriminate between single cells and cell aggregates or debris particles. Once single cells were selected based on brightfield images, mean intensity values from channel 02 (fluorescence) were plotted against mean intensity values from channel 04 (fluorescence). Annexin V-FITC positive (annexin V-FITC+/PI−) cells were classified as apoptotic cells, annexin V-FITC/PI double-positive (annexin V-FITC+/PI+) cells were classified as dead cells, and PI negative (PI-) cells as viable cells. Viability was calculated based on the proportion of PI negative cells from the total cell population, as shown in Fig. S1. The population of cells that were only PI positive (annexin V-FITC-/PI+, late apoptotic cells) were considered as dead cells, however this population was negligible (<1%) for all cell samples studied after all stress conditions.

2.7. Lactate dehydrogenase release assay

Cell membrane integrity was assessed by using a lactate dehydrogenase (LDH) release assay (CyQUANT; ThermoFisher, Waltham, USA). Loss of cell integrity was measured based on the level of LDH released upon damage to the plasma membrane. The assay is based on the conversion of lactate to pyruvate, which is catalyzed by LDH and results in formation of $NADH^+$. The tetrazolium salt included in the kit is reduced to formazan in presence of $NADH^+$ and can be quantified by absorbance measurements at 490 nm with a reference absorbance of 680 nm. Measurements were performed by using a Tecan Spark plate reader (Tecan, Männedorf, Switzerland). The total cell concentration was adjusted to ca. 150,000 cells/ml with RPMI medium (cell concentration to be within the linear range for this assay (data not shown)). Cells were incubated at 37 °C and 5% CO_2 for 45 min (with spiked water or Triton X-100) before the assay was carried out according to the manufactureŕs protocol. Release of the amount of LDH in the medium was calculated according to Eq. (1):

$$\text{LDH release } (\%) = \left(\frac{Spontanous\ \ LDH\ \ activity}{Maximum\ \ LDH\ \ activity}\right)*100 \quad (1)$$

Spontaneous LDH activity was based on measurements of cell suspensions spiked with water and maximum LDH activity values were derived from cell suspensions spiked with Triton X-100 to a target concentration of 10% (v/v). The results for each sample are based on measurements of four replicate wells.

3. Results

Jurkat cell suspensions were submitted to thawing at three defined temperatures, freeze-thawing in the presence of different DMSO concentrations and shaking in absence and presence of FBS. The stressed samples were characterized by using orthogonal methods for evaluation of the quality of cell suspensions.

3.1. FIM-CNN for measurement of cell counts, cell viability and debris particle concentration

We used FlowCam images of viable and dead cells as well as debris particles (Fig. 1A) to train a CNN for image classification. The recall value (proportion of positive identifications of all true positives present in the population) for classification of debris particles with our model was 99.5%, proving a high confidence of this classification approach (Fig. 1B). Similar recall values were achieved for the viable and dead cell populations (94.0% and 96.6%, respectively). For evaluation of the classification model performance, the F1 score is an additional metric used to assess the weighted average of the precision and recall. Here, the F1 score for debris, viable cells and dead cells was determined to be 0.991, 0.933 and 0.919, respectively. Such high values confirm the low number of incorrectly classified images during the testing phase of the networks fine-tuning. Therefore, FIM-CNN is presented in this study as a novel method for determination of the concentration of viable and dead cells, as well as for quantification of debris particles with a heterogeneous size distribution (Fig. 1C).

3.2. Effect of thawing temperature

Frozen Jurkat cell suspensions were thawed at 5 °C, 25 °C and 37 °C to evaluate the impact of thawing temperature on cell quality (Fig. 2A). FIM-CNN and automated cell counting showed an increase in recovery of viable cells with increasing thawing temperatures. Furthermore, FIM-CNN demonstrated a higher recovery of cells (viable and dead) in aliquots thawed at 37 °C ($1.4*10^6 \pm 0.1*10^6$ cells/ml) compared to aliquots which were thawed at 20 °C ($7.7*10^5 \pm 0.6*10^5$ cells/ml) and 5 °C ($9.7*10^5 \pm 1.1*10^5$ cells/ml).

Comparable concentrations of viable cells were obtained from both methods; however, the counts for dead cells and debris particles differed substantially. FIM-CNN measured a higher number of dead cells in samples thawed at 5 °C, as well as an increasing concentration of debris particles with decreasing thawing temperature. At the lowest tested thawing temperature of 5 °C, cell suspensions contained over $4x10^6$ debris particles/ml (i.e., 4-fold higher than the initial cell concentration), including dark and dense particles which were not observed in cell suspensions thawed at 37 °C and 20 °C (Fig. S2).

High cell viability was recorded for aliquots thawed at 37 °C and 20 °C (Fig. 2B). The two fluorescence-based methods showed a viability between 86% and 91%, whereas with FIM-CNN values were between 63% and 71%. However, a clear decrease in cell viability to 43%, 50% and 22% was observed for aliquots thawed at 5 °C according to the calcein-AM, PI and FIM-CNN assays, respectively. For all three thawing temperatures, there was a discrepancy in the absolute values of determined cell viability, when comparing the two fluorescence-based assays and FIM-CNN.

The annexin V-FITC assay suggests that cells are more likely to undergo apoptosis when thawed at lower temperatures (Fig. 2C). In

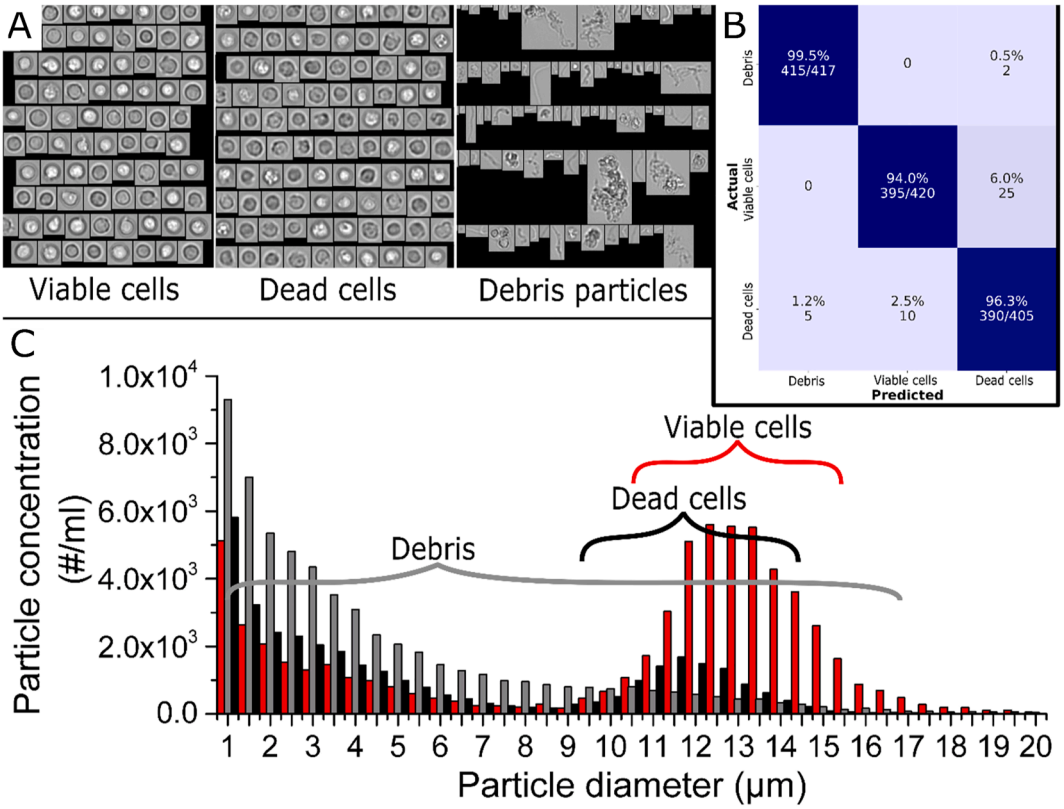

Fig. 1. (A) Examplery FlowCam images selected for training of the CNN model, (B) confusion matrix obtained from cross-validation analysis on image datasets not used during model training, (C) particle size distribution of cell suspensions vortexed (enriched in debris particles), heat treated (enriched in dead cells) and freshly thawed (viable cells) determined by using FlowCam.

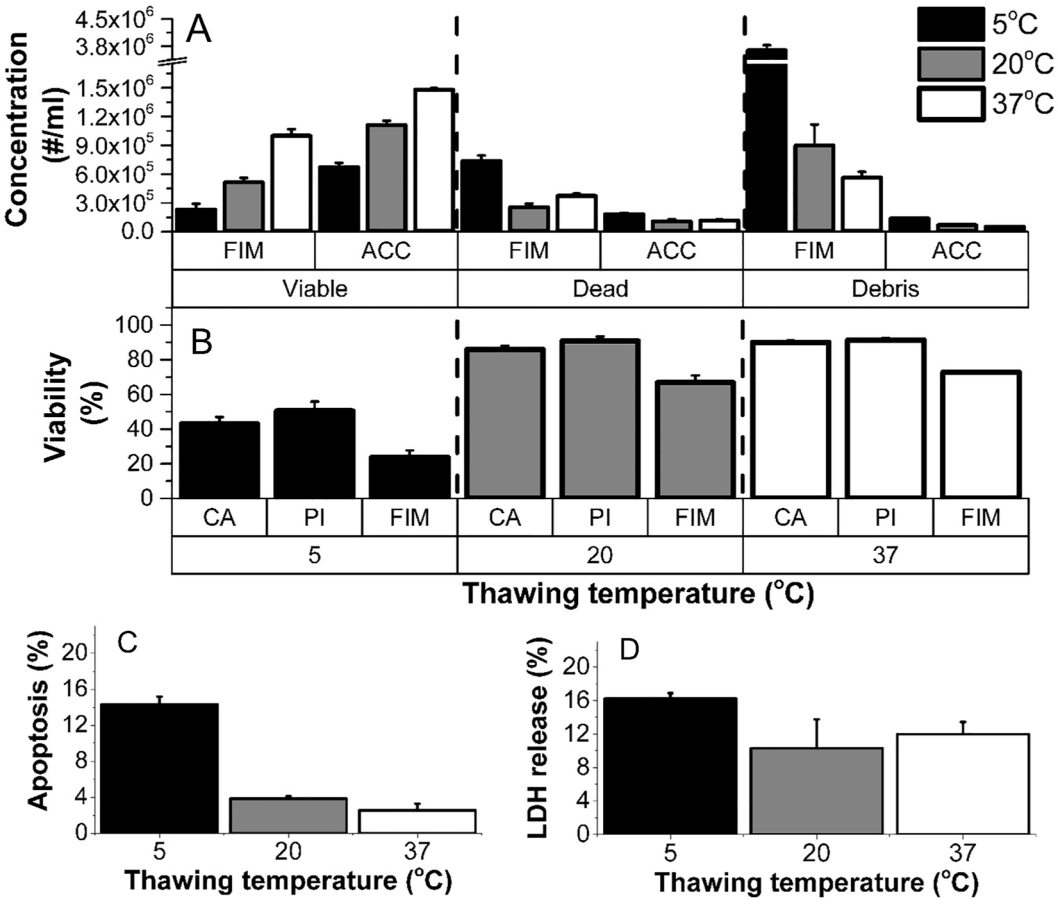

Fig. 2. Measurements of cell aliquots after thawing at 5 °C, 25 °C and 37 °C. (A) Determination of concentration of cellular debris, viable and dead cells measured by using FIM-CNN (FIM) and automated cell counting (ACC). (B) Measurement of cell viability by performing calcein-AM (CA), propiodium iodide (PI) and FIM-CNN assays. Assessment of (C) cell apoptosis with annexin V-FITC assay and (D) LDH release. Error bars represent standard deviations of mean values.

particular, a marked increase in apoptotic cells can be observed in cell suspensions thawed at 5 °C. The LDH release assay confirmed the detrimental effects of low thawing temperature on cells, albeit less pronounced (Fig. 2D).

3.3. Effect of freeze-thawing

Jurkat cells formulated in RPMI medium and DMSO (0%, 1%, 2.5%, 5% and 10% [v/v]) were submitted to one freeze–thaw cycle, which included storage of the cell suspensions at −18 °C for three hours and 2 min of thawing at 37 °C. Freeze-thawing of cell suspensions with 0% and 1% (v/v) DMSO led to a reduction of cell counts by > 98%, indicating that under these conditions practically all cells lose their viability (data not shown).

Concentrations of cells (viable and dead) and debris particles were determined by using FIM-CNN (Fig. 3A). With higher DMSO concentrations, higher total cell concentrations were observed after one freeze–thaw cycle, compared to lower tested cryoprotectant concentrations. Furthermore, cell suspensions with 10% (v/v) DMSO contained the lowest number of debris particles after freeze-thawing. Total cell concentrations prior to freezing (T0) and after three hours of storage at room temperature (Ctrl) were comparable for each tested DMSO concentration. However, control cell suspensions with 10% (v/v) DMSO showed slightly elevated debris contents compared to T0 and cell suspensions with lower DMSO content.

Interestingly, cell viability determined after freeze-thawing was heavily dependent on the assay used (Fig. 3C). The calcein-AM assay suggested the smallest changes of cell viability, with 85–90% cell viability, irrespective of DMSO content and time point. In contrast, PI and FIM-CNN assays showed noticeable (ca. 20%) losses in viability for cell suspensions frozen with 2.5% (v/v) DMSO, indicating that this concentration of cryoprotectant is insufficient for cell stabilization upon freezing. The PI assay also showed a smaller drop of ca. 10% in cell viability for cell suspensions with 5% and 10% (v/v) DMSO for freeze-thawed and control samples compared to T0, whereas FIM showed such a decrease in cell viability only for cell formulations containing 10% (v/v) DMSO. The toxic effects of DMSO was demonstrated by loss of cell viability after an exposure of 3 h at RT for each tested concentration according to the PI assay, and at 10% (v/v) based on FIM. Based on the results from PI and FIM, the best cell-stabilizing effect of DMSO was achieved at 5% (v/v).

An increase in LDH release in the medium was observed in cell suspensions which underwent freeze-thawing or were stored at room temperature in presence of DMSO (Fig. 4A). Only small differences in LDH concentration were observed in cell formulations with different DMSO concentrations. However, cells frozen with 5% (v/v) DMSO showed less LDH release compared to suspensions with 2.5% and 10% (v/v). Similarly, the fraction of apoptotic cells was smallest for cell suspensions with 5% (v/v) upon freeze-thawing (Fig. 4B).

3.4. Effect of shaking stress

Jurkat cell suspensions were submitted to horizontal shaking in presence and absence of 10% (v/v) FBS. Fig. 5A presents the total concentration of viable and dead cells, as well as debris particles measured by FIM-CNN in the two cell formulations at given time points. Following shaking stress, a substantial decrease in the total number of cells was observed in formulations without FBS compared to cell

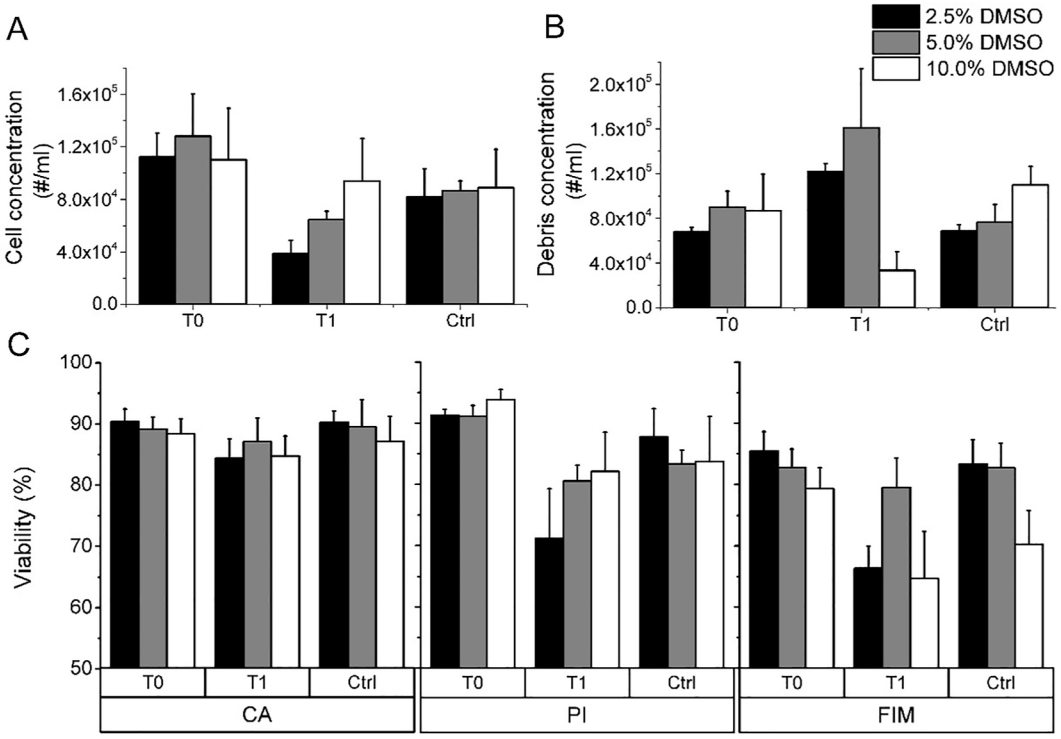

Fig. 3. Cell suspensions supplemented with DMSO at three different concentrations before (T0) and after a single freeze–thaw step following a storage for 3 h at either −18 °C (T1) or storage for 3 h at RT (Ctrl). FIM was used to measure the concentration of (A) total (viable + dead) cells and (B) debris particles. (C) Cell viability was deteremined by using calcein-AM (CA), propiodium iodide (PI) and FIM-CNN (FIM) assays. Error bars represent standard deviation of mean values.

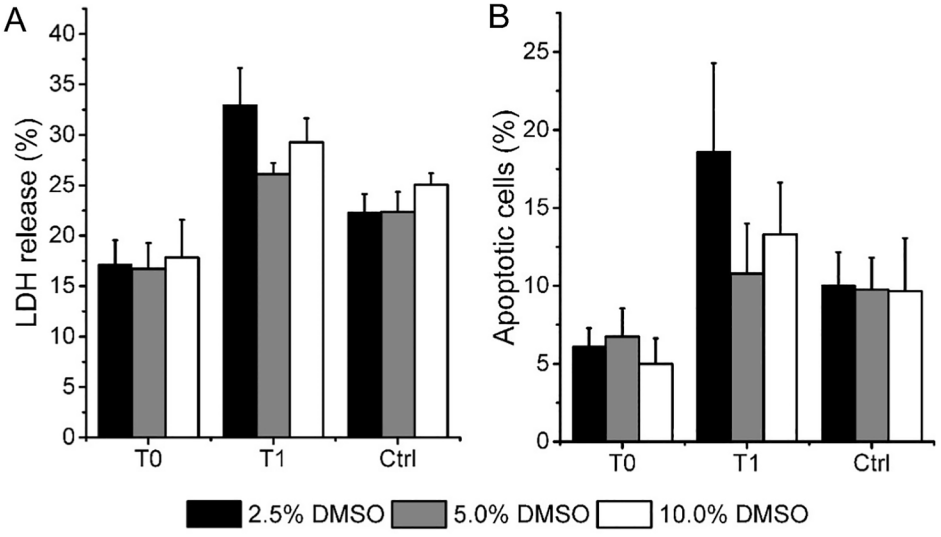

Fig. 4. Cell suspensions supplemented with DMSO at three different concentrations befire (T0) and after a single freeze–thaw step following a storage for 3 h at either −18 °C (T1) or storage for 3 h at RT (Ctrl). (A) LDH release assay and (B) apoptotic cell fraction quantified by using imaging flow cytometry (annexin V-FITC assay) at given time points. Error bars represent standard deviation of mean values.

suspensions containing FBS. A remarkable increase in concentration of debris particles was observed for both formulations. Notably, debris present in stressed cell suspensions supplemented with FBS originated not only from ruptured cells but also from aggregated proteins present in FBS (observed in stressed RPMI medium with 10% [v/v] FBS, data not shown). Cell viability after shaking stress and quiescent storage was very similar to the viability of cells at T0 according to all three methods used (Fig. S3).

The LDH release in stressed cell suspensions was higher compared to T0 or control cell suspensions, irrespective of FBS content. The increase in LDH release in the formulation with FBS was unexpected, given the observation that cell viability and cell concentration remained unchanged at all sampling points. A slight increase in the apoptotic cell fraction was observed after shaking in formulations with and without FBS, but a similar increase was observed in the unshaken control. Thus, shaking stress did not have a detectable impact on cell apoptosis in our study.

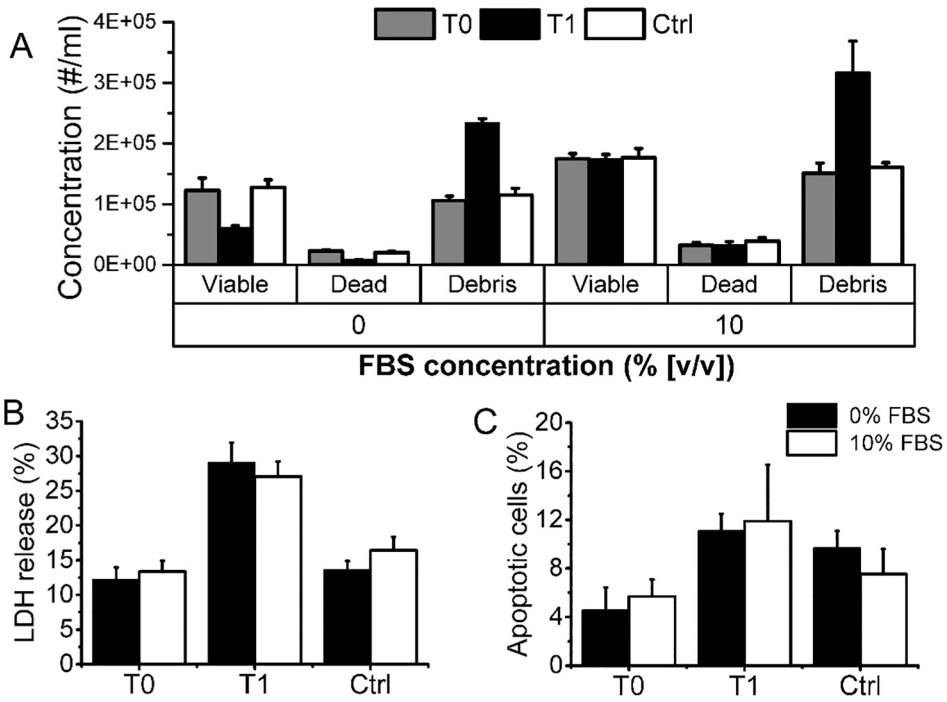

Fig. 5. . Cell suspensions without or with FBS (10% (v/v)) before (T0) and after shaking (T1) or quiescent storage (Ctrl) at room temperature. (A) Total concentration of cells (viable and dead) and debris particles by using FIM. (B) LDH release and (C) apoptotic cell fraction quantified by using imaging flow cytometry (annexin V-FITC assay) at given time points. Error bars represent standard deviation of mean values.

4. Discussion

Currently approved CBMPs are either stored in a cryopreserved (frozen liquid) or a non-frozen (liquid) state [25]. In both cases, cells may be exposed to all kind of stress factors, e.g., resulting from freeze-thawing or handling in the clinic prior to administration. This may cause cell damage, loss in quality and potential clinical implications, such as serious adverse effects or lack of drug efficacy. Cells have developed mechanisms to handle certain stress stimuli by activating signalling pathways and stress response proteins [6]. However, when the threshold of deleterious factors is surpassed, cells can abruptly lose membrane integrity or undergo programmed death [28]. Within human bodies, macrophages and dendritic cells of the innate immune system are equipped with appropriate mechanisms for removal of dying cells [17,23]. However, in CBMPs any cell degradants that may be formed, such as dead cells and cell debris, will remain within the product and might accelerate further cell degradation [25]. Furthermore, debris particles originating from abruptly ruptured cells are deficient in “eat-me” signals of apoptotic cells [29]. After administration, such dead cells and debris particles may trigger the immune system potentially resulting in inflammatory responses [17].

Viable cell concentration is considered as one of the most important quality attributes of CBMPs. A multitude of viability assays, based on the integrity of cell membrane or cellular metabolism, is available [30]. However, common viability assays involve fluorescent staining which encompass expensive fluorescent dyes and multistep preparation procedures with incubation times. Additionally, manual gating in flow cytometers is heavily biased and difficult to reproduce between different operators [31,32]. Thus, the drawbacks of these assays limit their capabilities to be robust and high-throughput methods for quantification of dead cells. Furthermore, classic trypan blue exclusion exhibits cytotoxic effects to cells [33], whereas other colorimetric assays can be affected by the pH of the culture medium or particular enzymes [30]. These drawbacks may compromise assay accuracy and precision.

In our study we applied FIM-CNN to accurately determine the number of viable and dead cells in suspensions of up to 200,000 cells/ml based on morphological appearance of cells. Cell death can be manifested by several morphological changes to the cell appearance, including rounding of the cell and cytoplasmic swelling [34]. These are not obvious in the FlowCam images to a human eye and are difficult to discriminate with the use of morphological parameters output by the FlowCam software [35]. However, pattern recognition algorithms implemented in CNN models have been shown to successfully discriminate between complex fingerprints, i.e., protein aggregate structures formed upon different stress conditions [36], and proved to be successful in classification of cell-related particles in our study.

The characterization of particulate matter in parenterals is described in pharmacopeial monographs and products should meet the acceptance limits for subvisible particle impurities sized above 10 μm and 25 μm [19]. However, given the particulate nature of cells, it is challenging to fulfil specific particle testing requirements applicable to injectable products, as human cells fall within the subvisible size range (typically 7–30 μm) [37]. One of the standard pharmacopeial methods for quantification of subvisible particle impurities, light obscuration, will not discriminate between cells and other particulates. Hence, high-throughput microscopy methods providing morphological data on particles within several hundred μl are promising tools for evaluation of particulates in cell-based products. Previously, the FIM approach was utilized to identify and quantify Dynabeads, which are commonly used during cell activation, in cell suspensions [26]. Moreover, FIM has also found its use in detection of other particulates, such as process impurities in CBMPs [13]. Here, by using FIM-CNN, reliable numbers on the concentration of debris particles sized 1–50 μm could be obtained (Fig. 1). Debris particles consist of a mixture of cell-derived lipids, proteins, nucleic acids and potentially other extrinsic particles, and thus are particulate impurities in CBMPs. In our study the debris population is less clearly defined than the different cell populations and can also consist of, e.g., aggregated FBS-derived proteins or other non-cell derived particles. Nevertheless, the FIM-CNN method showed the capability to monitor the levels of an entire debris particle population which may provide relevant information on the potential implications for product quality (consistency and stability) and safety of these drug

products (see discussion above). In addition, debris content imaged by using a bright-field microscope in cell suspensions was previously used to assess the level of late-stage apoptotic primary human hepatocytes and MDCK cells [38]. Similarly, we observed that exposure of cells to stress conditions led to an increase in cellular debris which correlated well with loss in cell viability and total cell count.

The unique supply chain of some CBMPs, where at least one freeze–thaw cycle is included, makes cryopreservation crucial in conserving the integrity of the product. Cryopreservation of human cells has been widely studied and multiple factors have been found critical in this process [39–42]. The freezing and thawing rates are two of the most critical parameters to be optimized to achieve high recovery of functional cells post-thawing. However, the optimal conditions are different for each cell suspension, and the impact of the thawing rate is less understood compared to the effect of freezing rate on cells [39]. Jurkat cells used in our study were submitted to controlled freezing with 10% (v/v) DMSO at a rate of 1 °C min^{-1}. Subsequent thawing at 5 °C in a water bath had deleterious effect on the viability and apoptotic rate of cells (Fig. 2). The negative impact of slow thawing on cells may result from recrystallization of ice. Metastable ice crystals formed during freezing may have formed larger crystals upon thawing at 5 °C, leading to denaturation of cellular proteins and disruption of membranes [43]. On the one hand, similar observations were made by Thorpe et al., who reported that decreasing the thawing temperature led to a lower survival of mouse lymphocytes [44]. On the other hand, our results differ from another study in which the thawing temperature had minimal effects on the survival of T cells [39]. The differences may originate not only from the different cell lines used in both studies but also from the different cell media. In addition to reduced viability, we observed an increase in concentration of debris particles at lower thawing temperatures with dense and irregular particles formed at the lowest thawing temperature (Fig. S2). Such debris particles were not observed in cell suspensions thawed at 20 °C or 37 °C.

The presence of cryoprotectants is important for the cryopreservation of cells stored at ultra-low temperatures (vapour phase of liquid nitrogen [<120 °C]). DMSO is currently the most widely used cryoprotectant in cryobiology [40]. Its amphiphilic and water-binding properties allow for a ready pass through cell membranes, thereby avoiding the efflux of water from the cytoplasm and thus preventing cellular dehydration upon freezing. At commonly used DMSO concentrations, such as 5–10% (v/v), formation of large intracellular and extracellular crystalline lattices is prevented by interfering with water molecules [45]. Formation of ice crystals and preservation of cell viability will also depend on the cooling rate, where the preferred very slow cooling rates (0.1 °C min^{-1}) produce fine dendritic ice structures and fast cooling rates (10 °C min^{-1}) generate large ice crystals [39]. In our study, Jurkat cells were subjected to passive (uncontrolled) freezing at −18 °C in presence of DMSO at a concentration ranging from 0% to 10% to mimic unintentional freezing. In agreement with previously reported data [46], the lowest tested DMSO concentrations (i.e., 0% and 1%) did not show any cryoprotection towards cells upon freeze-thawing as nearly a complete loss in cell viability was observed (data not shown). In contrast, the highest tested DMSO concentration of 10% (v/v) showed the highest cell recovery after one freeze–thaw cycle with the lowest number of debris particles present in cell suspensions (Fig. 3). Although, control samples (stored at RT) with the highest tested DMSO concentration showed an increase in debris particle over time, most likely due to its cytotoxic effect on cells.

Interestingly, the three viability assays used in our study did not provide conclusive results on the degree of protection against freeze-thawing at each tested DMSO concentration. The calcein-AM assay showed to be least sensitive in detecting changes in cell viability after freeze–thaw, whereas the PI and FIM assays detected a substantial drop in viability in suspensions with 2.5% (v/v) DMSO. However, for cell suspensions with 5% and 10% (v/v) DMSO, a reduced viability was observed with the PI assay for freeze-thawed and control samples, whereas FIM suggested minimal impact of freeze-thawing on cell viability with 5% (v/v) DMSO. It should be noted that each of the viability assays used may result in different outcomes given the different assay principles. For example, when using the calcein-AM assay, some apoptotic cells would be metabolically active and show positive staining, whereas others may be classified as dead cells. In the PI assay, only PI positive cells were classified as dead and cells undergoing early apoptosis did not show fluorescence, thus were regarded as viable. However, it is not currently possible to discriminate apoptotic cells by using FIM-CNN, therefore these cells may be classified to either the viable or dead cell population. In addition, post-thawed cell suspensions with 5% (v/v) DMSO showed the smallest fraction of apoptotic cells (based on annexin V-FITC assay) and the lowest LDH release, compared to the two other tested DMSO concentrations (Fig. 4). Similar observations were made for peripheral blood stem cells [47,48]. After cryopreservation with 5% DMSO, less apoptotic and dead peripheral blood stem cells compared to suspensions with 10% DMSO were measured [48]. The apoptosis-inducing effect of DMSO, via interaction with the PD-1 receptor and their ligands [40], was observed in our control group where a nearly 2-fold increase in apoptotic cell content was recorded. Taking into consideration the toxicity of DMSO and its potential to cause adverse effects upon administration [47], optimization of the DMSO concentration, or its replacement by a less cytotoxic alternative, should be an important focus during formulation development of cryopreserved CBMPs. Furthermore, effects of freeze-thawing on the functionality of cells and cellular biochemical pathways was beyond the scope of this study, but should also be tested during the development of CBMPs [25,49].

Mechanical stress is potentially the most frequent stress factor to which biopharmaceutical products are exposed to during processing, transportation and handling [50]. Solid-liquid and air–liquid interfaces play a crucial role in the formation of particles in protein-based formulations during agitation [51]. Thereby, amphiphilic, non-ionic surfactants (e.g., polysorbate 20 or 80) are commonly used in order to reduce protein aggregation upon interfacial stress and mechanical shock [52]. Unfortunately, such an approach may not be successful for CBMPs, as polysorbates have lytic effects on cells even at low concentrations [53]. Up to date, mild shaking conditions were applied to cell suspensions mainly for the purpose of cell expansion or to induce formation of cell aggregates for creation *ex vivo* tissue models [54,55]. In our study, we instigated harsher stress conditions to mimic potential “real-life” mechanical stress which has been shown to have detrimental effects on protein-based therapeutics [50,51]. Cell suspensions filled into cryovials and positioned vertically were unaffected by shaking speeds up to 500 rpm. However, positioning of the cryovials horizontally led to a dramatic loss (ca. 50%) of total cell concentration after relatively short shaking stress at 185 rpm (Fig. 5). Although the cell viability was unaffected by the mechanical stress according to the two fluorescence-based methods and FIM-CNN, LDH release and apoptosis were markedly increased compared to control samples. The increase in free LDH content suggests compromised cell quality and illustrates the value of using orthogonal cell characterization techniques. Furthermore, FBS demonstrated a protective effect towards cells upon shaking. While FBS is a commonly used supplement in cell culture and may be protective towards cells against mechanical stress, it is considered as a process-related impurity that is difficult to remove in the downstream processing steps [4]. Additionally, FBS is animal-derived, which is associated with safety and immunogenicity concerns. Moreover, bovine serum proteins are also susceptible to aggregation and may form particulate species, which add another unwanted complexity with respect to particulate impurities in CBMPs [19]. Ultimately, a wider array of formulation excipients should be tested in cell suspensions submitted to forced degradation studies in order to allow for a decision-based formulation strategy of CBMPs.

5. Conclusions

To the best of our knowledge, this study is the first to demonstrate the application of systematic forced degradation studies in the evaluation of cell stability and formulation, using Jurkat cells as model. The uniform cell line of immortalized cells may not fully reflect the behaviour of cell samples used in clinics. The aging of primary human cells will introduce a much greater heterogeneity on morphological cell features and pose greater challenges for acquisition of quality parameters. However, application of CNN for image classification allowed us to utilize FIM as a robust and fast analytical tool for characterization of cell suspensions, which has the potential for translation into assessment of "real-life" samples. Cell viability was assessed by using FIM-CNN in addition to other established approaches and a good correlation between the methods was observed. In addition, quantification of debris particles in CBMPs was only possible with FIM-CNN, highlighting the method's ability to monitor particulate impurities in cell suspensions. Overall, our study shows that thermal, freeze–thaw and shaking stresses are relevant tools for CBMP formulation studies. Moreover, it illustrates the importance of choosing a broad range of analytical methods to better understand the impact of each stress factor on CBMP quality.

Declaration of Competing Interest

The authors declare that they have no known competing financial interests or personal relationships that could have appeared to influence the work reported in this paper.

Acknowledgement

We thank Karin Hoogendoorn for her useful suggestions and critical review of the manuscript.

Appendix A. Supplementary material

Supplementary data to this article can be found online at https://doi.org/10.1016/j.ejpb.2021.07.004.

References

[1] G. Walsh, Biopharmaceutical benchmarks 2018, Nat. Biotechnol. 36 (12) (2018) 1136–1145, https://doi.org/10.1038/nbt.4305.
[2] J.E. Eyles, S. Vessillier, A. Jones, G. Stacey, C.K. Schneider, J. Price, Cell therapy products: focus on issues with manufacturing and quality control of chimeric antigen receptor T-cell therapies, J. Chem. Technol. Biotechnol. 94 (4) (2019) 1008–1016, https://doi.org/10.1002/jctb.5829.
[3] D. Jere, A.S. Sediq, J. Huwyler, I. Vollrath, M. Kardorff, H.-C. Mahler, Challenges for Cell-Based Medicinal Products From a Pharmaceutical Product Perspective, J. Pharm. Sci. (2020), https://doi.org/10.1016/j.xphs.2020.11.040.
[4] B.L. Levine, J. Miskin, K. Wonnacott, C. Keir, Global Manufacturing of CAR T Cell Therapy, Mol. Ther. Methods Clin. Dev. 4 (2017) 92–101, https://doi.org/10.1016/j.omtm.2016.12.006.
[5] E.M. Iancu, L.E. Kandalaft, Challenges and advantages of cell therapy manufacturing under Good Manufacturing Practices within the hospital setting, Curr. Opin. Biotechnol. 65 (2020) 233–241, https://doi.org/10.1016/j.copbio.2020.05.005.
[6] S. Fulda, A.M. Gorman, O. Hori, A. Samali, Cellular stress responses: cell survival and cell death, Int. J. Cell Biol. 2010 (2010), https://doi.org/10.1155/2010/214074.
[7] E.J. Woods, S. Thirumala, S.S. Badhe-Buchanan, D. Clarke, A.J. Mathew, Off the shelf cellular therapeutics: Factors to consider during cryopreservation and storage of human cells for clinical use, Cytotherapy. 18 (6) (2016) 697–711, https://doi.org/10.1016/j.jcyt.2016.03.295.
[8] D. Clarke, D. Harati, J. Martin, et al., Managing particulates in cellular therapy, Cytotherapy. 14 (9) (2012) 1032–1040, https://doi.org/10.3109/14653249.2012.706709.
[9] D. Clarke, J. Stanton, D. Powers, et al., Managing particulates in cell therapy: Guidance for best practice, Cytotherapy. 18 (9) (2016) 1063–1076, https://doi.org/10.1016/j.jcyt.2016.05.011.
[10] J.M. Marín Morales, N. Münch, K. Peter, et al., Automated Clinical Grade Expansion of Regulatory T Cells in a Fully Closed System, Front. Immunol. 10 (2019) 38, https://doi.org/10.3389/fimmu.2019.00038.
[11] A.A. Neurauter, M. Bonyhadi, E. Lien, et al., Cell isolation and expansion using Dynabeads, Adv. Biochem. Eng. Biotechnol. 106 (2007) 41–73, https://doi.org/10.1007/10_2007_072.
[12] R.K. Iyer, P.A. Bowles, H. Kim, A. Dulgar-Tulloch, Industrializing Autologous Adoptive Immunotherapies: Manufacturing Advances and Challenges, Front. Med. (Lausanne). 5 (2018) 150, https://doi.org/10.3389/fmed.2018.00150.
[13] I. Vollrath, R. Mathaes, A.S. Sediq, et al., Subvisible Particulate Contamination in Cell Therapy Products-Can We Distinguish? J. Pharm. Sci. (2019) https://doi.org/10.1016/j.xphs.2019.09.002.
[14] R.A. Morgan, B. Boyerinas, Genetic Modification of T Cells, Biomedicines 4 (2016) 2, https://doi.org/10.3390/biomedicines4020009.
[15] European Medicines Agency. Guideline on quality, non-clinical and clinical requirements for investigational advanced therapy medicinal products in clinical trials. 2019 https://www.ema.europa.eu/ documents/ scientific-guideline/draft-guideline-quality-non-clinical-clinical-requirements-investigational-advanced-therapy_en.pdf. Accessed 05.Mar.2021.
[16] C.A. Herberts, M.S.G. Kwa, H.P.H. Hermsen, Risk factors in the development of stem cell therapy, J. Transl. Med. 9 (1) (2011) 29, https://doi.org/10.1186/1479-5876-9-29.
[17] J. Westman, S. Grinstein, P.E. Marques, Phagocytosis of Necrotic Debris at Sites of Injury and Inflammation, Front. Immunol. 10 (2019) 3030, https://doi.org/10.3389/fimmu.2019.03030.
[18] D.R. Green, T. Ferguson, L. Zitvogel, G. Kroemer, Immunogenic and tolerogenic cell death, Nat. Rev. Immunol. 9 (5) (2009) 353–363, https://doi.org/10.1038/nri2545.
[19] J.F. Carpenter, T.W. Randolph, W. Jiskoot, et al., Overlooking subvisible particles in therapeutic protein products: gaps that may compromise product quality, J. Pharm. Sci. 98 (4) (2009) 1201–1205, https://doi.org/10.1002/jps.21530.
[20] S. Bukofzer, J. Ayres, A. Chavez, et al., Industry Perspective on the Medical Risk of Visible Particles in Injectable Drug Products, PDA J. Pharm. Sci. Tech. 69 (1) (2015) 123, https://doi.org/10.5731/pdajpst.2015.01037.
[21] A. Hawe, M. Wiggenhorn, M. van de Weert, J.H.O. Garbe, H.-C. Mahler, W. Jiskoot, Forced Degradation of Therapeutic Proteins, J. Pharm. Sci. 101 (3) (2012) 895–913, https://doi.org/10.1002/jps.22812.
[22] J. Halley, Y.R. Chou, C. Cicchino, et al., An Industry Perspective on Forced Degradation Studies of Biopharmaceuticals: Survey Outcome and Recommendations, J. Pharm. Sci. 109 (1) (2020) 6–21, https://doi.org/10.1016/j.xphs.2019.09.018.
[23] C. Ammann, Stability studies needed to define the handling and transport conditions of sensitive pharmaceutical or biotechnological products, AAPS PharmSciTech. 12 (4) (2011) 1264–1275, https://doi.org/10.1208/s12249-011-9684-0.
[24] European Medicines Agency. Guideline on quality, non-clinical and clinical aspects of medicinal products containing genetically modified cells. 2020. https://www.ema.europa.eu/documents/scientific-guideline/guideline-quality-non-clinical-clinical-aspects-medicinal-products-containing-genetically-modified_en.pdf. Accessed 03.Mar.2021.
[25] K.H. Hoogendoorn, D.J.A. Crommelin, W. Jiskoot, Formulation of Cell-Based Medicinal Products: A Question of Life or Death? J. Pharm. Sci. (2020) https://doi.org/10.1016/j.xphs.2020.07.002.
[26] A.D. Grabarek, E. Senel, T. Menzen, et al., Particulate impurities in cell-based medicinal products traced by flow imaging microscopy combined with deep learning for image analysis, Cytotherapy. (2020), https://doi.org/10.1016/j.jcyt.2020.04.093.
[27] O. Russakovsky, J. Deng, H. Su, et al., ImageNet Large Scale Visual Recognition Challenge, Int. J. Comput. Vis. 115 (3) (2015) 211–252, https://doi.org/10.1007/s11263-015-0816-y.
[28] D.R. Green, F. Llambi, Cell Death Signaling, Cold Spring Harb Perspect. Biol. 7 (12) (2015), https://doi.org/10.1101/cshperspect.a006080.
[29] M. Sachet, Y.Y. Liang, R. Oehler, The immune response to secondary necrotic cells, Apoptosis 22 (10) (2017) 1189–1204, https://doi.org/10.1007/s10495-017-1413-z.
[30] O. Kepp, L. Galluzzi, M. Lipinski, J. Yuan, G. Kroemer, Cell death assays for drug discovery, Nat Rev Drug Discov. 10 (3) (2011) 221–237, https://doi.org/10.1038/nrd3373.
[31] M. Lippeveld, C. Knill, E. Ladlow, et al., Classification of Human White Blood Cells Using Machine Learning for Stain-Free Imaging Flow Cytometry, Cytometry A. (2019), https://doi.org/10.1002/cyto.a.23920.
[32] R. Grant, K. Coopman, N. Medcalf, et al., Quantifying Operator Subjectivity within Flow Cytometry Data Analysis as a Source of Measurement Uncertainty and the Impact of Experience on Results, PDA J. Pharm. Sci. Tech. 75 (1) (2021) 33, https://doi.org/10.5731/pdajpst.2019.011213.
[33] L.L.-Y. Chan, W.L. Rice, J. Qiu, Observation and quantification of the morphological effect of trypan blue rupturing dead or dying cells, PLoS ONE. 15 (1) (2020) e0227950, https://doi.org/10.1371/journal.pone.0227950.
[34] T. Vanden Berghe, N. Vanlangenakker, E. Parthoens, et al., Necroptosis, necrosis and secondary necrosis converge on similar cellular disintegration features, Cell Death Differ. 17 (6) (2010) 922–930, https://doi.org/10.1038/cdd.2009.184.
[35] A.S. Sediq, R. Klem, M.R. Nejadnik, P. Meij, W. Jiskoot, Label-Free, Flow-Imaging Methods for Determination of Cell Concentration and Viability, Pharm. Res. 35 (8) (2018) 150, https://doi.org/10.1007/s11095-018-2422-5.
[36] A. Gambe-Gilbuena, Y. Shibano, E. Krayukhina, T. Torisu, S. Uchiyama, Automatic Identification of the Stress Sources of Protein Aggregates Using Flow Imaging Microscopy Images, J. Pharm. Sci. 109 (1) (2020) 614–623, https://doi.org/10.1016/j.xphs.2019.10.034.

[37] G. Rosenberg, Microscopic Haematology : A Practical Guide for the Laboratory, Harwood Academic Publishers, Amsterdam, 1997.
[38] M. Ölander, N. Handin, P. Artursson, Image-Based Quantification of Cell Debris as a Measure of Apoptosis, Anal Chem. (2019) 5548–5552, https://doi.org/10.1021/acs.analchem.9b01243.
[39] J. Baboo, P. Kilbride, M. Delahaye, et al., The Impact of Varying Cooling and Thawing Rates on the Quality of Cryopreserved Human Peripheral Blood T Cells, Sci. Rep. 9 (1) (2019) 3417, https://doi.org/10.1038/s41598-019-39957-x.
[40] J.M. Baust, L.H. Campbell, J.W. Harbell, Best practices for cryopreserving, thawing, recovering, and assessing cells, Vitro Cell Dev. Biol. Anim. 53 (10) (2017) 855–871, https://doi.org/10.1007/s11626-017-0201-y.
[41] S.M. Hughes, Z. Shu, C.N. Levy, et al., Cryopreservation of Human Mucosal Leukocytes, PLoS One 11 (5) (2016), https://doi.org/10.1371/journal.pone.0156293.
[42] K. Hornberger, G. Yu, D. McKenna, A. Hubel, Cryopreservation of Hematopoietic Stem Cells: Emerging Assays, Cryoprotectant Agents, and Technology to Improve Outcomes, Transfus Med. Hemother. 46 (3) (2019) 188–196, https://doi.org/10.1159/000496068.
[43] P. Mazur, S. Seki, Survival of mouse oocytes after being cooled in a vitrification solution to -196°C at 95° to 70,000°C/min and warmed at 610° to 118,000°C/min: A new paradigm for cryopreservation by vitrification, Cryobiology 62 (1) (2011) 1–7, https://doi.org/10.1016/j.cryobiol.2010.10.159.
[44] P. Thorpe, S. Knight, J. Farrant, Optimal conditions for the preservation of mouse lymph node cells in liquid nitrogen using cooling rate techniques, Cryobiology. 13 (1976) 126–133.
[45] C.F. Brayton, Dimethyl sulfoxide (DMSO): a review, Cornell Vet. 76 (1) (1986) 61–90.
[46] A. Giugliarelli, P. Sassi, L. Urbanelli, et al., Cryopreservation of cells: FT-IR monitoring of lipid membrane at freeze-thaw cycles, Biophys Chem. 208 (2016) 34–39, https://doi.org/10.1016/j.bpc.2015.08.001.
[47] I. Mitrus, A. Smagur, W. Fidyk, et al., Reduction of DMSO concentration in cryopreservation mixture from 10% to 7.5% and 5% has no impact on engraftment after autologous peripheral blood stem cell transplantation: results of a prospective, randomized study, Bone Marrow Transplant. 53 (3) (2018) 274–280, https://doi.org/10.1038/s41409-017-0056-6.
[48] J. Abrahamsen, et al. Cryopreserving human peripheral blood progenitor cells with 5-percent rather than 10-percent DMSO results in less apoptosis and necrosis in CD34+cells.
[49] S.R. Panch, S.K. Srivastava, N. Elavia, et al., Effect of Cryopreservation on Autologous Chimeric Antigen Receptor T Cell Characteristics, Mol. Ther. (2019) 1275–1285, https://doi.org/10.1016/j.ymthe.2019.05.015.
[50] M.R. Nejadnik, T.W. Randolph, D.B. Volkin, et al., Postproduction Handling and Administration of Protein Pharmaceuticals and Potential Instability Issues, J. Pharm. Sci. 107 (8) (2018) 2013–2019, https://doi.org/10.1016/j.xphs.2018.04.005.
[51] T.K. Das, L.O. Narhi, A. Sreedhara, et al., Stress Factors in mAb Drug Substance Production Processes: Critical Assessment of Impact on Product Quality and Control Strategy, J. Pharm. Sci. 109 (1) (2020) 116–133, https://doi.org/10.1016/j.xphs.2019.09.023.
[52] A.D. Grabarek, U. Bozic, J. Rousel, et al., What Makes Polysorbate Functional? Impact of Polysorbate 80 Grade and Quality on IgG Stability During Mechanical Stress, J. Pharm. Sci. (2019), https://doi.org/10.1016/j.xphs.2019.10.015.
[53] M.G. Moleirinho, S. Rosa, M.J.T. Carrondo, et al., Clinical-Grade Oncolytic Adenovirus Purification Using Polysorbate 20 as an Alternative for Cell Lysis, Curr Gene Ther. 18 (6) (2018) 366–374, https://doi.org/10.2174/1566523218666181109141257.
[54] W. Klöckner, J. Büchs, Advances in shaking technologies, Trends Biotechnol. 30 (6) (2012) 307–314, https://doi.org/10.1016/j.tibtech.2012.03.001.
[55] E. Kim, J.C. Kim, K. Min, M. Goh, G. Tae, Rapid and Versatile Cell Aggregate Formation Using Lipid-Conjugated Heparin, ACS Appl. Mater Interfaces. 10 (29) (2018) 24431–24439, https://doi.org/10.1021/acsami.8b07731.